analytical chemistry

Article

Cite This: *Anal. Chem.* XXXX, XXX, XXX−XXX

pubs.acs.org/ac

21 Tesla FT-ICR Mass Spectrometer for Ultrahigh-Resolution Analysis of Complex Organic Mixtures

Donald F. Smith,[†] David C. Podgorski,[†,‡,§] Ryan P. Rodgers,[†,∥] Greg T. Blakney,[†] and Christopher L. Hendrickson*[,†,∥]

[†]National High Magnetic Field Laboratory, Florida State University, 1800 East Paul Dirac Drive, Tallahassee, Florida 32310, United States

[‡]Department of Earth, Ocean and Atmospheric Science, Florida State University, P.O. Box 3064520, Tallahassee, Florida 32306, United States

[∥]Department of Chemistry and Biochemistry, Florida State University, 95 Chieftain Way, Tallahassee, Florida 32303, United States

ABSTRACT: We describe complex organic mixture analysis by 21 tesla (T) Fourier transform ion cyclotron resonance mass spectrometry (FT-ICR MS). Ultrahigh mass-resolving power ($m/\Delta m_{50\%}$ > 2 700 000 at m/z 400) and mass accuracy (80 ppb rms) enable resolution and confident identification of tens of thousands of unique elemental compositions. We demonstrate 2.2-fold higher mass-resolving power, 2.6-fold better mass measurement accuracy, and 1.3-fold more assigned molecular formulas compared to our custom-built, state-of-the-art 9.4 T FT-ICR mass spectrometer for petroleum and dissolved organic matter (DOM) analyses. Analysis of a heavy petroleum distillate exemplifies the need for ultrahigh-performance mass spectrometry (49 040 assigned molecular formulas for 21 T versus 29 012 for 9.4 T) and extends the identification of previously unresolved O_o, S_sO_o, and NO_o classes. Mass selective ion accumulation (20 Thompson isolation) of an asphalt volcano sample yields 462 resolved mass spectral peaks at m/z 677 and reveals previously unresolved $C_cH_hN_nO_oS_s$ mass differences at high mass (m/z > 600). Similar performance gains are realized in the analysis of dissolved organic matter, where doubly charged O_o species are resolved from singly charged SO_o species, which requires a mass-resolving power greater than 1 400 000 (at m/z 600). This direct comparison reveals the continued need for higher mass-resolving power and better mass accuracy for comprehensive molecular characterization of the most complex organic mixtures.

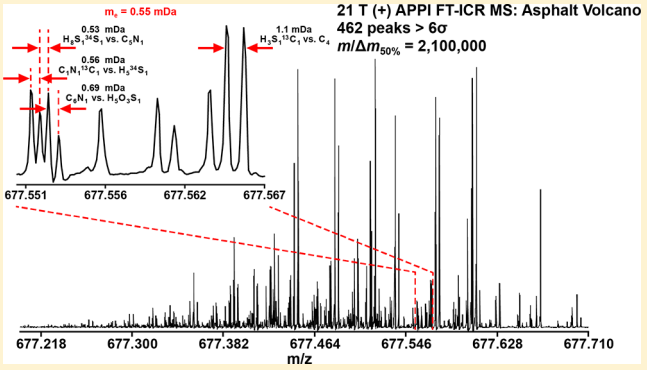

Fourier transform ion cyclotron resonance (FT-ICR) mass spectrometry[1] has become the method of choice for detailed chemical characterization of natural complex mixtures. The high mass-resolving power, mass accuracy, and dynamic range of FT-ICR enable resolution and confident elemental formula assignment for tens of thousands of unique components in complex organic mixtures.[2,3] Electrospray ionization (ESI)[4] and atmospheric pressure photoionization (APPI)[5] provide efficient ionization of polar and nonpolar components and are easily interfaced with FT-ICR. Petroleum crude oils have been studied extensively by FT-ICR,[2,6,7] as well as oil sands,[8,9] bio-oils,[10] and dissolved organic matter.[3,11,12] Specific components isolated by wet chemistry or chromatography have also been investigated, including asphaltenes,[13,14] acidic fractions,[15] interfacial species,[16] aromatic ring fractions,[17] and metal porphyrins.[18]

Instrumentation advances over the past 20 years have significantly increased the breadth and depth of compositional information obtained by high-resolution FT-ICR mass spectrometry, as recently reviewed by Cho et al.[19] Briefly, harmonization of the trapping electric field has improved spectral performance.[20−23] Controlled ejection of ions from an external multipole trap has reduced m/z discrimination during ion transfer to the ICR cell, which increases the accessible m/z range for broadband analysis.[24] Radial distribution of the postexcitation ion cyclotron radius has reduced space charge interactions for improved dynamic range and improved transient lifetime (i.e., higher mass-resolving power) for less-abundant species.[25] Multiple frequency detection allows for higher mass-resolving power on any existing FT-ICR, as demonstrated recently by Cho et al., who achieved a mass-resolving power of 1 500 000 (at m/z 400) on a 7 T FT-ICR.[26] However, multiple-frequency detection generally decreases sensitivity and induces signals at unwanted frequencies, which complicates spectral interpretation. Broadband phase correction for absorption mode display improves mass-resolving power and mass accuracy for any FT-ICR transient.[23,27−29] In addition, the high-field Orbitrap ($m/\Delta m_{50\%}$ = 480 000 at m/z

Received: October 10, 2017
Accepted: December 21, 2017

DOI: 10.1021/acs.analchem.7b04159
Anal. Chem. XXXX, XXX, XXX−XXX

400) has been used to analyze lighter crude oils with low sulfur content.[30] Extension of the time-domain transient ($m/\Delta m_{50\%}$ = 960 000 at m/z 400), in combination with spectral stitching, shows that the 3.4 mDa mass difference (C_3 versus S_1H_4) can be resolved at m/z 1070; however, smaller mass differences (e.g., 1.1 mDa, C_4 vs $S_1H_3{}^{13}C_1$) are not resolved.

FT-ICR mass-resolving power and spectral acquisition rate improve linearly, while mass accuracy and dynamic range improve quadratically with increasing magnetic field strength.[31] This is especially important for heavy petroleum mixtures, such as heavy feedstocks, high boiling point distillates, and asphaltenes, because the compositional complexity demands high mass-resolving power, mass accuracy, and dynamic range over a wide m/z range. We recently reported the design and initial performance of the National High Magnetic Field Laboratory (NHMFL) 21 T (T) FT-ICR mass spectrometer, the highest magnetic field available to date for FT-ICR.[32,33] Here, we present complex mixture characterization on the newly developed NHMFL 21 T FT-ICR mass spectrometer, which features the latest developments in ICR cell technology and ion storage/transfer methodologies for complex mixture analysis. Performance improvement over a previous state-of-the-art 9.4 T FT-ICR MS for complex mixtures is demonstrated. Over 49 000 unique chemical species are identified at ultrahigh mass-resolving power (>2.7 million at m/z 400) with broadband root-mean-square (rms) mass measurement accuracy less than 80 parts-per-billion (ppb).

EXPERIMENTAL METHODS

Solvents. High-performance liquid chromatography (HPLC)-grade methanol and toluene were purchased from J.T Baker Chemicals (Phillipsburg, NJ). Glacial acetic acid and ammonium hydroxide were purchased from Sigma-Aldrich (St. Louis, MO), and tetramethylammonium hydroxide (TMAH, 25 wt % in MeOH) was purchased from Acros Organics (Fair Law, NJ).

Samples. A broad range of samples with different origins and complexities was selected. Suwanee River fulvic acid (SRFA; 1S101F, International Humic Substances Society) is a black water system containing dissolved organic matter (DOM) that is similar in composition to that found in the major carbon exporting rivers (e.g., Amazon and Congo). As of 2016, DOM from the Suwannee River was used in >780 published studies that have been cited >30 000 times. National Institutes of Standards and Technology (NIST, Gaithersburg, MD) Standard Reference Material 2779 Gulf of Mexico Crude Oil was collected directly from the Macondo well during the response to the Deepwater Horizon oil spill of 2010. It is used as a quality control material for ongoing research into the environmental impact of the Deepwater Horizon oil spill. Similarly, NIST Standard Reference Material 2777 Weathered Gulf of Mexico Oil is a field weathered residue from the Deepwater Horizon oil spill of 2010. An asphalt volcano sample (*Il Duomito*) is from a 35 000 year old naturally occurring petroleum seep in the Santa Barbara Basin, CA.[34] It is a dense asphalt that is heavily weathered and extremely complex. Canadian bitumen is a heavily biodegraded crude oil, which is chemically complex (high heteroatom content). It also presents many challenges in production, transport, and refining. The deasphalted Canadian bitumen heavy distillate is the most chemically complex distillate fraction of crude oil. This fraction presents many challenges for oil refining because of its high heteroatom content and aromaticity.

Negative-Ion-Mode ESI. SRFA was diluted to a final concentration of 100 μg/mL in methanol. NIST Standard Reference Material 2777 Weathered Gulf of Mexico Oil was diluted to a final concentration of 250 μg/mL in 50:50 methanol/toluene with 1% (v/v) ammonium hydroxide solution added to aid deprotonation. Canadian bitumen and a deasphalted Canadian bitumen heavy distillation cut (523−593 °C) were diluted to final concentrations of 250 μg/mL in 50:50 methanol/toluene with 0.125% (v/v) TMAH solution added to aid deprotonation. Samples were analyzed by micro-ESI at an infusion rate of 0.5 μL/min.

Positive-Ion-Mode ESI. NIST Standard Reference Material 2779 Gulf of Mexico Crude Oil was diluted to a final concentration of 250 μg/mL in 50:50 methanol/toluene with 1% (v/v) acetic acid solution added to aid protonation. Samples were analyzed by micro-ESI at an infusion rate of 0.5 μL/min.

Positive-Ion-Mode APPI. Deasphalted Canadian bitumen heavy distillation cut (523−593 °C) and a naturally occurring asphalt volcano seep (*Il Duomito*) were diluted to a final concentration of 50 μg/mL and infused into an Ion Max NG ion source equipped with a krypton VUV lamp for APPI at a rate of 50 μL/min.

Mass Spectrometry and Data Analysis. All samples were analyzed in triplicate by 9.4 T FT-ICR MS[35] and 21 T FT-ICR MS.[32] Ions were initially accumulated in an external multipole ion guide (9.4 T: 200−1,000 ms, 21 T: 1−5 ms) and released m/z-dependently by decrease of an auxiliary radio frequency potential between the multipole rods and the end-cap electrode.[24] Ions were excited to m/z-dependent radius to maximize the dynamic range and number of observed mass spectral peaks (m/z 200−1500; 9.4 T: 25−47%, 21 T: 32−64%),[25] and excitation and detection were performed on the same pair of electrodes.[36] The seven-segment compensated open cylindrical ICR cell in the 9.4 T FT-ICR is operated with 0.75−1 V trapping potential,[21,35] and the dynamically harmonized ICR cell in the 21 T FT-ICR is operated with 6 V trapping potential.[20,32] Time-domain transients of 6.8 (9.4 T) and 6.3 (21 T) seconds were acquired with the Predator data station, with 100 time-domain acquisitions averaged for all experiments.[37] For 21 T FT-ICR MS, the Predator data station handled excitation and detection only, which were initiated by a TTL trigger from the commercial Thermo data station. We combine the data stations because use of Predator excitation and detection produces a more easily phased mass spectrum. Mass spectra were phase-corrected[27] and internally calibrated with a high-abundance homologous series based on the "walking" calibration method.[38] Peaks with signal magnitude greater than 6 times the baseline root-mean-square (rms) noise at m/z 500 were exported to peak lists, and molecular formula assignments and data visualization were performed with PetroOrg © software.[39] Molecular formula assignments with an error >0.5 parts-per-million (ppm) were discarded, and only chemical classes with a combined relative abundance ≥0.25% of the total were considered.

RESULTS AND DISCUSSION

The move to upgrade heavier, more heteroatom-rich crude oils and residuals into useable feedstocks demands high-performance mass spectrometry to characterize the chemical constituents in these highly complex mixtures. The depletion of light, low sulfur crude oil has resulted in a global shift toward production and refinement of these relatively heavy, acidic, and high sulfur crude oils. Heteroatoms (N, O, S, V, Ni) in these

DOI: 10.1021/acs.analchem.7b04159
Anal. Chem. XXXX, XXX, XXX−XXX

heavy oils and their distillate fractions are problematic in upstream and downstream processes with respect to deposition, corrosion, catalyst poisoning, and emulsion formation. The mass spectra of samples collected from problematic locations in the petroleum stream from production to refinement are typically very complex and/or shifted to high m/z. Therefore, the increase in mass-resolving power and mass measurement accuracy afforded by 21 T FT-ICR MS are essential to advance molecular-level knowledge of problematic compounds and to develop strategies to mitigate their negative impact.

Even greater performance is required for asphaltenes, which are a highly polar, aromatic, and heteroatom-rich fraction of crude oil defined by their insolubility in *n*-heptane. Deposition of asphaltenes during offshore production alone can result in economic losses of up to $1.2 million per day.[40] Previous analyses of asphaltene polar compounds by ESI FT-ICR MS show that they are composed of polydisperse combinations of O_o, N_nO_o, S_sO_o, N_nS_s, and $N_nO_oS_s$, heteroatom classes.[41−43] Highly condensed polycyclic aromatic hydrocarbons and nonpolar heteroatom containing compounds with O_o, N_n, S_s and vanadium or nickel are observed in asphaltenes analyzed by APPI.[44−48] Asphaltenes are an extremely complex and problematic fraction of petroleum that necessitates higher performance mass spectrometry for proper characterization.

Environmentally weathered crude oils and asphalts contain additional oxidized transformation products, which presents even more challenge, especially when nitrogen and sulfur are also present in the mixture.[49,50] Species with high oxygen atom content appear with increased relative abundance in field deposits and emulsions.[16,51] Emulsions can be encountered in each stage of petroleum production and processing. Most emulsions form unintentionally, but those formed in production by steam-assisted gravity drainage or water flooding are desired to reduce the viscosity of heavy crude oils.[52,53] Recent advances in isolation and characterization of interfacial material have revealed that species responsible for emulsion stabilization contain higher order O_o and S_sO_o compounds (where $o \geq 2$) that consist of mono- and poly functional acids.[16,54,55] Ultrahigh-resolution mass spectrometry is necessary to ensure proper assignment of highly oxygenated, singly- and multiply charged peaks for identification of problematic surface active species, and continued advances in high-resolution mass spectrometry are necessary.

We chose seven samples with a range of complexities to evaluate the performance of the 21 T FT-ICR mass spectrometer for complex mixture analysis. Figure 1 shows the number of molecular formula assignments for the NHMFL 9.4 T versus 21 T FT-ICR MS. The 21 T FT-ICR instrument yields more molecular formula assignments for all samples except the Gulf of Mexico crude oil, for which the assignments are equal to within experimental variation. We believe this is because the heteroatom content in the Gulf of Mexico crude oil is limited to nitrogen and sulfur (i.e., low oxygen content), so the 3.4 mDa mass difference between C_3 and S_1H_4 is the smallest frequently encountered mass difference that must be resolved, due to relatively low heteroatom class diversity. In this case, the 9.4 T FT-ICR MS resolves the 3.4 mDa mass difference across the mass spectrum, so there are few unresolved species.

As molecular complexity increases, the analytical demands placed on the mass spectrometer also increase. In addition, different ionization methods yield different ions that can complicate the mass spectrum. Negative-ion mode ESI, which

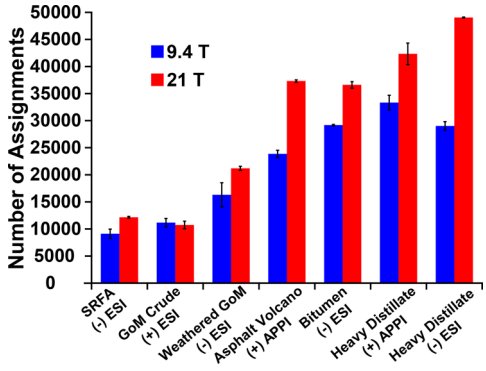

Figure 1. Number of assigned molecular formulas for the NHMFL 9.4 T versus 21 T FT-ICR mass spectrometer (mean ± 1 SD, 100 time-domain averaged transients).

targets acidic oxygen and neutral (pyrrolic) nitrogen species, yields greater heteroatom class complexity and thus smaller mass differences that are resolved at 21 T, but not at 9.4 T (see below). Oxygen further complicates the heteroatom space, because molecules with $C_cH_hN_nO_oS_s$ add additional closely spaced ions that are more difficult to resolve at higher m/z, as exemplified by a mass difference of 1.79 mDa (H_3O_3 versus $C_2N_1{}^{13}C_1$). APPI introduces an additional challenge, because both protonated and radical ions are generated, which gives rise to a common 1.1 mDa mass difference (C_4 vs $S_1H_3{}^{13}C_1$) that can be difficult to resolve at high m/z at 9.4 T, as illustrated by the increase in the number of molecular formula assignments for APPI at 21 T. Compounded with high oxygen content (heavy oils, asphaltenes, etc.), APPI of complex mixtures requires higher performance mass spectrometry for proper chemical speciation. Thus, improvement in mass-resolving power results in improved chemical speciation. Further, higher field strength allows more ions to be trapped in the 21 T ICR cell before the onset of peak coalescence, which improves mass spectral performance for highly complex samples (see below). These improvements are observed as additional molecular formula assignments, and additional assignments of ^{13}C isotopologues, which can be used to confirm molecular ion formula assignments.

Mass measurement accuracy (rms of all assigned molecular formulas) improved >2-fold for all samples for 21 versus 9.4 T, as shown in Figure 2. This provides more confident assignment of molecular formulas and facile identification of incorrect

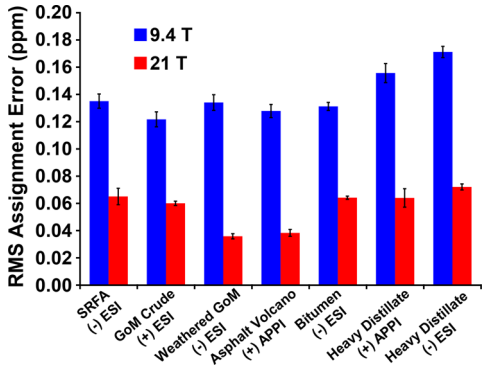

Figure 2. Root-mean-square assignment error for the NHMFL 9.4 T versus 21 T FT-ICR mass spectrometer (mean ± 1 SD, 100 time-domain averaged transients).

DOI: 10.1021/acs.analchem.7b04159
Anal. Chem. XXXX, XXX, XXX−XXX

assignments. Improved mass accuracy at high m/z, where residual mass error is larger, is especially important for heavy petroleum samples to ensure correct molecular formula assignment. As shown in Figure 1, the 21 T FT-ICR yields more molecular formula assignments than at 9.4 T. The rms mass measurement accuracy improves, despite the low signal-to-noise ratio (S/N) of many of the additional species identified at 21 T. Thus, the 21 T FT-ICR MS enables assignment of more molecular formulas at a higher confidence level than the 9.4 T instrument. We note that for ESI analysis of the least complex sample (light GOM crude oil, which has low heteroatom content), the ultrahigh mass-resolving power of the 21 T instrument does not increase the number of assigned molecular formulas. We suspect that this sample is sufficiently characterized by the 9.4 T mass spectrometer (i.e., no new species are resolved), but with reduced assignment confidence because of lower mass measurement accuracy.

As shown in Figures 1 and 2, the 21 T FT-ICR demonstrates the expected improvement on mass-resolving power and mass accuracy. A concomitant improvement in dynamic range is also expected, but the 21 and 9.4 T instruments yield mass spectra with similar S/N. Mitigating factors that may preclude observation of improved dynamic range include different ICR cell size (the 9.4 T ICR cell is larger than the 21 T ICR cell and thus has a greater ion storage capacity[22]) and different collisional damping rate of the ICR signal. Postexcitation ion kinetic energy scales quadratically with magnetic field, so ions at 21 T have ~5-fold higher kinetic energy than those at 9.4 T, and collisions with neutrals at high postexcitation radius can be detrimental to ICR signal lifetime, which would result in loss of detected signal magnitude (i.e., reduced S/N and dynamic range). This is an active area of investigation, and we anticipate that additional performance improvements will be realized once the limiting factors are identified and addressed.

Negative-ion ESI of a deasphalted heavy distillate at 21 T shows significant performance gains over 9.4 T and is an exemplary case for the value of higher field FT-ICR MS for heavy petroleum analysis, with a 1.7× improvement in the number of molecular formulas assigned and a 2.4× improvement in rms mass measurement accuracy. A mass measurement error histogram is shown in Figure 3 for 100 signal averaged time-domain transients from each instrument. Both distributions are centered at zero, but the 21 T distribution is 2-fold narrower. The 9.4 T distribution is broader and tails to negative error. Figure 4 shows the number of assignments versus heteroatom class for 9.4 versus 21 T for the same sample (negative-ion ESI of a deasphalted heavy distillate). Unique molecular formula assignments are highlighted by lighter colored bars. Unique assignments from the 9.4 T instrument occur mostly at low m/z (m/z 200–400), which we attribute to slightly better low m/z transmission versus the 21 T. However, a much larger number of unique assignments are observed at 21 T, especially for heteroatom classes with three or more oxygen atoms; N_1O_3, N_1O_4, N_1O_5, $N_1O_3S_1$, $N_1O_4S_1$, S_1O_3, S_1O_4, S_1O_5, S_2O_3, O_3, O_4, O_5 and O_6. In total, 11 685 unique monoisotopic molecular formulas are assigned on the 21 T. These unique assignments result largely from the ability to resolve a mass difference of 1.79 mDa (H_3O_3 versus $C_2N_1{}^{13}C_1$) across the entire m/z range. This performance enhancement will directly benefit the analysis of samples enriched in oxygen, such as weathered crude oils, asphalts, and emulsions.

Figure 5 (bottom) shows isoabundance-contoured double bond equivalents (DBE; number of rings plus double bonds to carbon) versus carbon number for the O_3 class. The compositional space of the O_3 class is truncated for the 9.4 T, whereas the 21 T reveals species that extend to higher carbon number and DBE, albeit with the loss of lower carbon number species. The mass scale-expanded inset at the top of Figure 5 shows m/z 769, where the 21 T resolves two ions with a mass difference of 1.79 mDa, but only a single peak is detected at 9.4 T. The required mass-resolving power to resolve a 1.79 mDa mass difference at m/z 769 is 430 000, which should be attainable at 9.4 T with a transient duration of 6.8 s. However, the large ion populations (due to high spectral complexity) can lead to space charge induced peak coalescence or loss of ion coherence, which results in the apparent loss of resolution shown in Figure 5. The number of ions that can be stored in the FT-ICR cell before the onset of peak coalescence increases quadratically with magnetic field, which enables large ion populations of extremely complex mixtures to be measured at 21 T with high sensitivity, ultrahigh mass-resolving power, and high mass measurement accuracy over a wide m/z range.

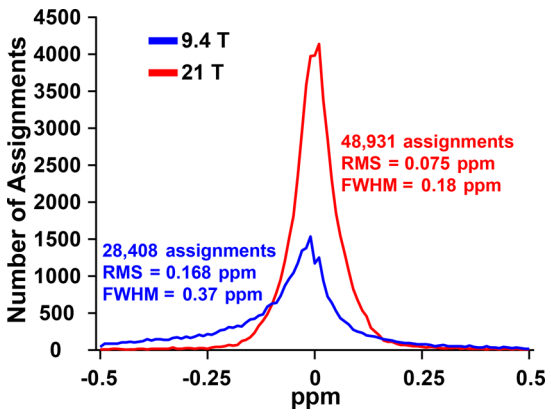

Figure 3. Measured mass error distribution from (−) ESI FT-ICR MS of a Canadian bitumen deasphalted heavy distillate (523–593 °C) with TMAH modifier for the NHMFL 9.4 T versus 21 T FT-ICR mass spectrometer (100 time-domain averaged transients). Mass errors were grouped into 10 ppb bins and plotted as the total number of molecular formulas assigned per bin.

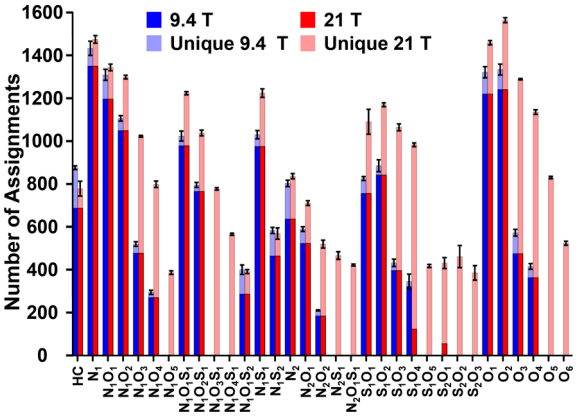

Figure 4. Number of assigned molecular formulas from (−) ESI FT-ICR MS of a Canadian bitumen deasphalted heavy distillate (523–593 °C) with TMAH modifier for the NHMFL 9.4 T versus 21 T FT-ICR MS (mean ±1 SD, 100 time-domain averaged transients). Lighter color bars represent unique molecular formula assignments.

DOI: 10.1021/acs.analchem.7b04159
Anal. Chem. XXXX, XXX, XXX–XXX

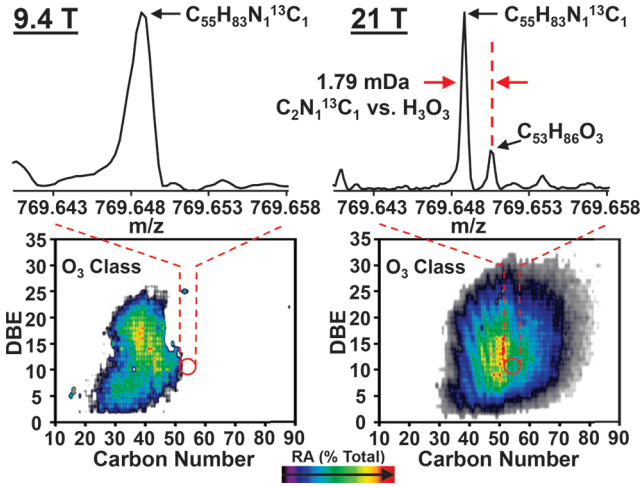

Figure 5. Mass scale expanded segment of (−) ESI FT-ICR mass spectra of a Canadian bitumen deasphalted heavy distillate (523−593 °C) with TMAH modifier (top) and isoabundance-contoured plots of DBE versus number of carbons for members of the O_3 class (bottom) from the NHMFL 9.4 T (left) and 21 T (right), both 100 time-domain averaged transients.

Figure 6 illustrates extremely high dynamic range (588:1 versus 18:1 for broadband mass analysis) for a 20 Thompson

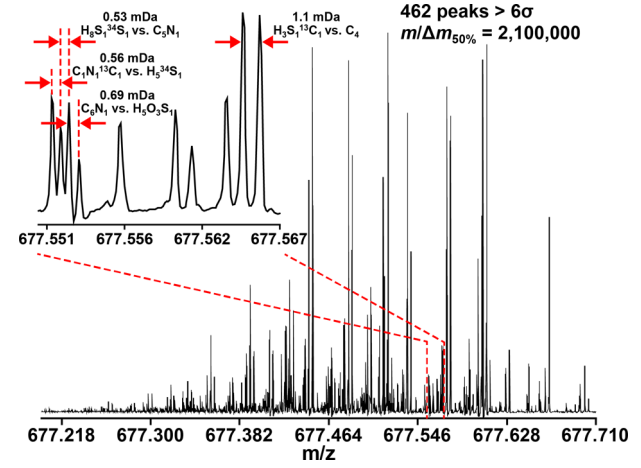

Figure 6. Mass scale expanded segment of the (+) APPI FT-ICR mass spectrum (200 time-domain averaged transients) of an asphalt volcano sample at m/z 677 after ion trap isolation of a 20 Th segment. Inset illustrates the need for ultrahigh mass-resolving power to resolve ions with a mass difference on the order of the mass of an electron (m_e = 0.55 mDa).

ion trap isolation from APPI of a highly weathered asphalt volcano sample collected from the seafloor off the coast of Santa Barbara, CA (m/z 674 ± 10 Th; 200 averaged transients). The narrow mass window enables a larger number of ions of interest to be analyzed while minimizing detrimental space charge effects.[56−58] To the best of our knowledge, this is the largest number of mass spectral peaks resolved and detected at a single nominal mass, with 462 peaks >6σ. Molecular formulas have been assigned to 83% of these detected peaks. The zoom inset highlights the spectral complexity in a 0.016 Da segment. The common 1.1 mDa mass difference (C_4 vs $S_1H_3{}^{13}C_1$) observed in APPI is baseline resolved, and the cluster of four peaks on the left demonstrate the need for ultrahigh mass-resolving power. Mass differences of 0.56 mDa ($C_1N_1{}^{13}C_1$ vs $H_5{}^{34}S_1$), 0.53 mDa ($H_8S_1{}^{34}S_1$ vs C_5N_1), and 0.69 mDa (C_6N_1 vs $H_5O_3S_1$) are resolved and identified. As discussed above, the combination of $C_cH_hN_nO_oS_s$ heteroatoms and radical/protonated ions generated from APPI present a model case for the need for the highest performance mass spectrometry available.

Application of ultrahigh-resolution mass spectrometry to answer complex questions regarding the composition and transformation of natural organic matter has steadily increased over the past two decades, since Novoty et al. demonstrated its utility in 1995 using laser desorption ionization, followed by Fievre et al. using electrospray ionization in 1997.[59,60] The molecular-level composition of DOM and changes in composition as a result of biogeochemical processes have been determined by FT-ICR MS for many types of aquatic environments, which include lakes, rivers, estuaries, and oceans.[61−68] Dissolved organic matter comprises a diverse array of O_o, N_nO_o, S_sO_o, and P_pO_o heteroatom classes. Molecular formulas containing O_o are the most abundant signals in a typical negative-ion ESI mass spectrum of DOM, with other heteroatom-containing species at much lower abundance. In addition, multiply charged ions at low abundance further complicate DOM mass spectra.[69,70] The high mass-resolving power and mass measurement accuracy of the 21 T FT-ICR MS provide unprecedented capability of resolving these species and confident assignment of molecular formulas.

Figure 7 shows mass expanded zoom insets of mass spectra of SRFA collected at 9.4 T (blue) and 21 T (red). A mass

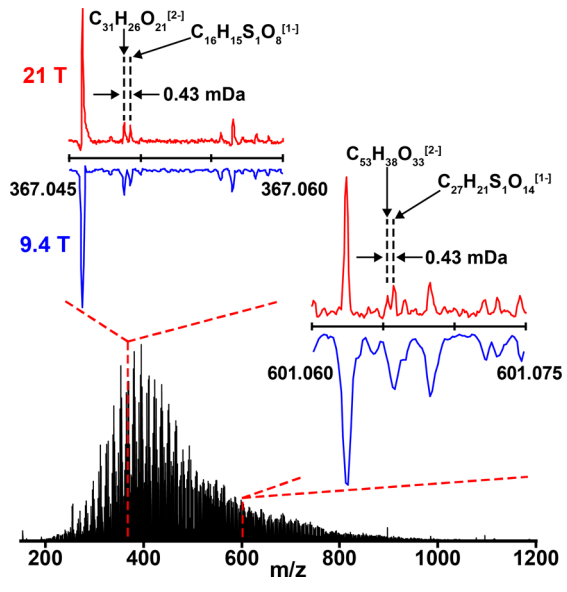

Figure 7. Mass scale expanded segment of (−) ESI FT-ICR mass spectrum of Suwannee River fulvic acid. Insets at m/z 367 and 601 show resolution of a 0.43 mDa mass difference, which results from a doubly charged oxygen containing ion and a singly charged sulfur containing ion. This difference can be resolved at low m/z at 9.4 T, but it requires the high mass-resolving power of 21 T to be resolved at higher m/z.

spacing of 0.43 mDa is observed at m/z 367, which had been observed previously,[33] and we identify as the difference between a doubly charged ion with a composition of $C_{31}H_{26}O_{21}{}^{[2-]}$, and singly charged ion, $C_{16}H_{15}S_1O_8{}^{[1-]}$, and can be resolved at m/z 367 by both 9.4 and 21 T. However, the

DOI: 10.1021/acs.analchem.7b04159
Anal. Chem. XXXX, XXX, XXX−XXX

high mass-resolving power at 21 T is required to resolve these species at m/z 601 ($C_{53}H_{38}O_{33}^{[2-]}$ versus $C_{27}H_{21}S_1O_{14}^{[1-]}$). The high mass-resolving power of 21 T is required to correctly assign multiply charged ions across the m/z range, and to properly assign sulfur containing species.

Often, conclusions about biogeochemical processes pertaining to entire regions, continents, oceans, or even the globe are modeled from samples collected at a specific place and time. Naturally, concerns arise regarding the amount of spatial and temporal resolution required to build accurate models for large-scale geochemical processes. The move to higher magnetic field and advancements in data processing have increased FT-ICR MS sample throughput dramatically. The 21 T FT-ICR MS provides the highest sample throughput to date. Routine analysis of DOM samples is completed with 3.1 s time-domain transients, which enables a full broadband mass spectrum to be collected every 10 min (100 averaged time-domain transients) with a mass-resolving power greater than 1.7 million at m/z 400. This high-throughput capability is at the forefront of a paradigm shift in spatial and temporal resolution to understand large-scale biogeochemical processes.

CONCLUSIONS

The NHMFL 21 T FT-ICR mass spectrometer exhibits predicted improvements in mass accuracy and mass-resolving power over our 9.4 T mass spectrometer. More molecular formulas are assigned at higher confidence level, at ultrahigh mass-resolving power, and with large ion populations. Performance improvement for heavy petroleum analysis illustrates the need for high magnetic field for thorough chemical characterization. The 21 T FT-ICR will play a prominent role to advance our understanding of heavy oils (and associated distillates), asphaltenes, emulsions, and dissolved organic matter. The instrument is available to all qualified users as part of the NSF High Field FT-ICR Mass Spectrometry User Facility.

AUTHOR INFORMATION

Corresponding Author

*Phone: (850)-644-0711. Fax: (850)-644-1366. E-mail: hendrick@magnet.fsu.edu.

ORCID

Donald F. Smith: 0000-0003-3331-0526

Ryan P. Rodgers: 0000-0003-1302-2850

Present Address

[§]D.C.P.: Pontchartrain Institute for Environmental Sciences, Department of Chemistry, University of New Orleans, 2000 Lakeshore Drive, New Orleans, LA 70148, United States

Notes

The authors declare no competing financial interest.

ACKNOWLEDGMENTS

This work was supported by NSF Division of Materials Research (DMR-11-57490), the State of Florida, and the Florida State University Future Fuels Institute.

REFERENCES

(1) Marshall, A. G.; Hendrickson, C. L.; Jackson, G. S. *Mass Spectrom. Rev.* **1998**, *17*, 1−35.

(2) Marshall, A. G.; Rodgers, R. P. *Proc. Natl. Acad. Sci. U. S. A.* **2008**, *105*, 18090−18095.

(3) Stenson, A. C.; Marshall, A. G.; Cooper, W. T. *Anal. Chem.* **2003**, *75*, 1275−1284.

(4) Fenn, J.; Mann, M.; Meng, C.; Wong, S.; Whitehouse, C. *Science* **1989**, *246*, 64−71.

(5) Robb, D. B.; Covey, T. R.; Bruins, A. P. *Anal. Chem.* **2000**, *72*, 3653−3659.

(6) Panda, S. K.; Andersson, J. T.; Schrader, W. *Anal. Bioanal. Chem.* **2007**, *389*, 1329−1339.

(7) Rodgers, R. P.; McKenna, A. M. *Anal. Chem.* **2011**, *83*, 4665−4687.

(8) Smith, D. F.; Schaub, T. M.; Kim, S.; Rodgers, R. P.; Rahimi, P.; Teclemariam, A.; Marshall, A. G. *Energy Fuels* **2008**, *22*, 2372−2378.

(9) Headley, J. V.; Barrow, M. P.; Peru, K. M.; Fahlman, B.; Frank, R. A.; Bickerton, G.; McMaster, M. E.; Parrott, J.; Hewitt, L. M. *Rapid Commun. Mass Spectrom.* **2011**, *25*, 1899−1909.

(10) Michailof, C. M.; Kalogiannis, K. G.; Sfetsas, T.; Patiaka, D. T.; Lappas, A. A. *WIREs Energy Environ.* **2016**, *5*, 614.

(11) Kujawinski, E. B.; Del Vecchio, R.; Blough, N. V.; Klein, G. C.; Marshall, A. G. *Mar. Chem.* **2004**, *92*, 23−37.

(12) Nebbioso, A.; Piccolo, A. *Anal. Bioanal. Chem.* **2013**, *405*, 109−124.

(13) McKenna, A. M.; Marshall, A. G.; Rodgers, R. P. *Energy Fuels* **2013**, *27*, 1257−1267.

(14) Chacón-Patiño, M. L.; Vesga-Martínez, S. J.; Blanco-Tirado, C.; Orrego-Ruiz, J. A.; Gómez-Escudero, A.; Combariza, M. Y. *Energy Fuels* **2016**, *30*, 4550−4561.

(15) Rowland, S. M.; Robbins, W. K.; Corilo, Y. E.; Marshall, A. G.; Rodgers, R. P. *Energy Fuels* **2014**, *28*, 5043−5048.

(16) Jarvis, J. M.; Robbins, W. K.; Corilo, Y. E.; Rodgers, R. P. *Energy Fuels* **2015**, *29*, 7058−7064.

(17) Podgorski, D. C.; Corilo, Y. E.; Nyadong, L.; Lobodin, V. V.; Bythell, B. J.; Robbins, W. K.; McKenna, A. M.; Marshall, A. G.; Rodgers, R. P. *Energy Fuels* **2013**, *27*, 1268−1276.

(18) Putman, J. C.; Rowland, S. M.; Corilo, Y. E.; McKenna, A. M. *Anal. Chem.* **2014**, *86*, 10708−10715.

(19) Cho, Y.; Ahmed, A.; Islam, A.; Kim, S. *Mass Spectrom. Rev.* **2015**, *34*, 248−263.

(20) Boldin, I. A.; Nikolaev, E. N. *Rapid Commun. Mass Spectrom.* **2011**, *25*, 122−126.

(21) Tolmachev, A. V.; Robinson, E. W.; Wu, S.; Kang, H.; Lourette, N. M.; Pasa-Tolic, L.; Smith, R. D. *J. Am. Soc. Mass Spectrom.* **2008**, *19*, 586−597.

(22) Kaiser, N. K.; Savory, J. J.; McKenna, A. M.; Quinn, J. P.; Hendrickson, C. L.; Marshall, A. G. *Anal. Chem.* **2011**, *83*, 6907−6910.

(23) Qi, Y.; Witt, M.; Jertz, R.; Baykut, G.; Barrow, M. P.; Nikolaev, E. N.; O'Connor, P. B. *Rapid Commun. Mass Spectrom.* **2012**, *26*, 2021−2026.

(24) Kaiser, N. K.; Savory, J. J.; Hendrickson, C. L. *J. Am. Soc. Mass Spectrom.* **2014**, *25*, 943−949.

(25) Kaiser, N. K.; McKenna, A. M.; Savory, J. J.; Hendrickson, C. L.; Marshall, A. G. *Anal. Chem.* **2013**, *85*, 265−272.

(26) Cho, E.; Witt, M.; Hur, M.; Jung, M.-J.; Kim, S. *Anal. Chem.* **2017**, *89*, 12101−12107.

(27) Xian, F.; Hendrickson, C. L.; Blakney, G. T.; Beu, S. C.; Marshall, A. G. *Anal. Chem.* **2010**, *82*, 8807−8812.

(28) Qi, Y.; Barrow, M. P.; Li, H.; Meier, J. E.; Van Orden, S. L.; Thompson, C. J.; O'Connor, P. B. *Anal. Chem.* **2012**, *84*, 2923−2929.

(29) Cho, Y.; Qi, Y.; O'Connor, P. B.; Barrow, M. P.; Kim, S. *J. Am. Soc. Mass Spectrom.* **2014**, *25*, 154−157.

(30) Zhurov, K. O.; Kozhinov, A. N.; Tsybin, Y. O. *Energy Fuels* **2013**, *27*, 2974−2983.

(31) Marshall, A. G.; Guan, S. *Rapid Commun. Mass Spectrom.* **1996**, *10*, 1819−1823.

(32) Hendrickson, C. L.; Quinn, J. P.; Kaiser, N. K.; Smith, D. F.; Blakney, G. T.; Chen, T.; Marshall, A. G.; Weisbrod, C. R.; Beu, S. C. *J. Am. Soc. Mass Spectrom.* **2015**, *26*, 1626−1632.

(33) Shaw, J. B.; Lin, T.-Y.; Leach, F. E.; Tolmachev, A. V.; Tolić, N.; Robinson, E. W.; Koppenaal, D. W.; Paša-Tolić, L. *J. Am. Soc. Mass Spectrom.* **2016**, *27*, 1929−1936.

(34) Valentine, D. L.; Reddy, C. M.; Farwell, C.; Hill, T. M.; Pizarro, O.; Yoerger, D. R.; Camilli, R.; Nelson, R. K.; Peacock, E. E.; Bagby, S.

DOI: 10.1021/acs.analchem.7b04159
Anal. Chem. XXXX, XXX, XXX−XXX

C.; Clarke, B. A.; Roman, C. N.; Soloway, M. *Nat. Geosci.* **2010**, *3*, 345−348.
(35) Kaiser, N. K.; Quinn, J. P.; Blakney, G. T.; Hendrickson, C. L.; Marshall, A. G. *J. Am. Soc. Mass Spectrom.* **2011**, *22*, 1343−1351.
(36) Chen, T.; Beu, S. C.; Kaiser, N. K.; Hendrickson, C. L. *Rev. Sci. Instrum.* **2014**, *85*, 066107.
(37) Blakney, G. T.; Hendrickson, C. L.; Marshall, A. G. *Int. J. Mass Spectrom.* **2011**, *306*, 246−252.
(38) Savory, J. J.; Kaiser, N. K.; McKenna, A. M.; Xian, F.; Blakney, G. T.; Rodgers, R. P.; Hendrickson, C. L.; Marshall, A. G. *Anal. Chem.* **2011**, *83*, 1732−1736.
(39) Corilo, Y. E. *PetroOrg Software*; Florida State University, Omics LLC: Tallahassee, FL, 2014.
(40) Creek, J. L. *Energy Fuels* **2005**, *19*, 1212−1224.
(41) Klein, G. C.; Kim, S.; Rodgers, R. P.; Marshall, A. G.; Yen, A.; Asomaning, S. *Energy Fuels* **2006**, *20*, 1965−1972.
(42) Smith, D. F.; Klein, G. C.; Yen, A. T.; Squicciarini, M. P.; Rodgers, R. P.; Marshall, A. G. *Energy Fuels* **2008**, *22*, 3112−3117.
(43) Wang, S. S.; Yang, C.; Xu, C. M.; Zhao, S. Q.; Shi, Q. *Sci. China: Chem.* **2013**, *56*, 856−862.
(44) Qian, K.; Mennito, A. S.; Edwards, K. E.; Ferrughelli, D. T. *Rapid Commun. Mass Spectrom.* **2008**, *22*, 2153−2160.
(45) Purcell, J. M.; Merdrignac, I.; Rodgers, R. P.; Marshall, A. G.; Gauthier, T.; Guibard, I. *Energy Fuels* **2010**, *24*, 2257−2265.
(46) Pereira, T. M. C.; Vanini, G.; Oliveira, E. C. S.; Cardoso, F. M. R.; Fleming, F. P.; Neto, A. C.; Lacerda, V.; Castro, E. V. R.; Vaz, B. G.; Romao, W. *Fuel* **2014**, *118*, 348−357.
(47) Zhao, X.; Shi, Q.; Gray, M. R.; Xu, C. M. *Sci. Rep.* **2014**, *4*, 5373.
(48) Chacón-Patiño, M. L.; Blanco-Tirado, C.; Orrego-Ruiz, J. A.; Gómez-Escudero, A.; Combariza, M. Y. *Energy Fuels* **2015**, *29*, 6330−6341.
(49) Ruddy, B. M.; Huettel, M.; Kostka, J. E.; Lobodin, V. V.; Bythell, B. J.; McKenna, A. M.; Aeppli, C.; Reddy, C. M.; Nelson, R. K.; Marshall, A. G.; Rodgers, R. P. *Energy Fuels* **2014**, *28*, 4043−4050.
(50) Chen, H.; Hou, A.; Corilo, Y. E.; Lin, Q.; Lu, J.; Mendelssohn, I. A.; Zhang, R.; Rodgers, R. P.; McKenna, A. M. *Environ. Sci. Technol.* **2016**, *50*, 9061−9069.
(51) Juyal, P.; Mapolelo, M. M.; Yen, A.; Rodgers, R. P.; Allenson, S. J. *Energy Fuels* **2015**, *29*, 2342−2350.
(52) Ashrafi, M.; Souraki, Y.; Torsaeter, O. *Energy Environment Research* **2012**, *2*, 140−156.
(53) Aichele, C. P.; Chapman, W. G.; Rhyne, L. D.; Subramani, H. J. *Exp. Therm. Fluid Sci.* **2014**, *53*, 190−196.
(54) Clingenpeel, A. C.; Robbins, W. K.; Corilo, Y. E.; Rodgers, R. P. *Energy Fuels* **2015**, *29*, 7150−7155.
(55) Clingenpeel, A. C.; Rowland, S. M.; Corilo, Y. E.; Zito, P.; Rodgers, R. P. *Energy Fuels* **2017**, *31*, 5933−5939.
(56) Southam, A. D.; Payne, T. G.; Cooper, H. J.; Arvanitis, T. N.; Viant, M. R. *Anal. Chem.* **2007**, *79*, 4595−4602.
(57) Gaspar, A.; Schrader, W. *Rapid Commun. Mass Spectrom.* **2012**, *26*, 1047−1052.
(58) Smith, D. F.; McKenna, A. M.; Corilo, Y. E.; Rodgers, R. P.; Marshall, A. G.; Heeren, R. M. A. *Energy Fuels* **2014**, *28*, 6284−6288.
(59) Novotny, F. J.; Rice, J. A.; Weil, D. A. *Environ. Sci. Technol.* **1995**, *29*, 2464−2466.
(60) Fievre, A.; Solouki, T.; Marshall, A. G.; Cooper, W. T. *Energy Fuels* **1997**, *11*, 554−560.
(61) Hertkorn, N.; Benner, R.; Frommberger, M.; Schmitt-Kopplin, P.; Witt, M.; Kaiser, K.; Kettrup, A.; Hedges, J. I. *Geochim. Cosmochim. Acta* **2006**, *70*, 2990−3010.
(62) Chipman, L.; Podgorski, D.; Green, S.; Kostka, J.; Cooper, W.; Huettel, M. *Limnol. Oceanogr.* **2010**, *55*, 857−871.
(63) Stubbins, A.; Hood, E.; Raymond, P. A.; Aiken, G. R.; Sleighter, R. L.; Hernes, P. J.; Butman, D.; Hatcher, P. G.; Striegl, R. G.; Schuster, P.; Abdulla, H. A. N.; Vermilyea, A. W.; Scott, D. T.; Spencer, R. G. M. *Nat. Geosci.* **2012**, *5*, 198−201.
(64) Jaffé, R.; Yamashita, Y.; Maie, N.; Cooper, W. T.; Dittmar, T.; Dodds, W. K.; Jones, J. B.; Myoshi, T.; Ortiz-Zayas, J. R.; Podgorski, D. C.; Watanabe, A. *Geochim. Cosmochim. Acta* **2012**, *94*, 95−108.
(65) Kellerman, A. M.; Kothawala, D. N.; Dittmar, T.; Tranvik, L. J. *Nat. Geosci.* **2015**, *8*, 454−457.
(66) Wagner, S.; Jaffé, R.; Cawley, K.; Dittmar, T.; Stubbins, A. *Frontiers in Chemistry* **2015**, *3*, 66.
(67) Mead, R. N.; Felix, J. D.; Avery, G. B.; Kieber, R. J.; Willey, J. D.; Podgorski, D. C. *Atmos. Environ.* **2015**, *105*, 162−168.
(68) Hodgkins, S. B.; Tfaily, M. M.; Podgorski, D. C.; McCalley, C. K.; Saleska, S. R.; Crill, P. M.; Rich, V. I.; Chanton, J. P.; Cooper, W. T. *Geochim. Cosmochim. Acta* **2016**, *187*, 123−140.
(69) Brown, T. L.; Rice, J. A. *Anal. Chem.* **2000**, *72*, 384−390.
(70) Gaspar, A.; Kunenkov, E. V.; Lock, R.; Desor, M.; Perminova, I.; Schmitt-Kopplin, P. *Rapid Commun. Mass Spectrom.* **2009**, *23*, 683−688.

DOI: 10.1021/acs.analchem.7b04159
Anal. Chem. XXXX, XXX, XXX−XXX